International Journal of Minerals, Metallurgy and Materials
Volume 26, Number 3, March 2019, Page 282
https://doi.org/10.1007/s12613-019-1736-6

Austenite grain growth of medium-carbon alloy steel with aluminum additions during heating process

Zi-yi Liu[1)], *Yan-ping Bao*[1)], *Min Wang*[1)], *Xin Li*[1)], *and Fan-zheng Zeng*[2)]

1) State key Laboratory of Advanced Metallurgy, University of Science and Technology Beijing, Beijing 100083, China
2) Xiangtan Iron & Steel Co., Ltd. of Hunan Valin, Xiangtan 411101, China
(Received: 18 June 2018; revised: 13 August 2018; accepted: 29 August 2018)

Abstract: In this study, the effects of heating temperature (850–1100°C) and holding time (30–150 min) on the grain growth behavior of austenite in medium-carbon alloy steel were investigated by conducting experiments. The abnormal grain growth and mixed grain structure phenomenon are explained using an equilibrium precipitation phase diagram calculated by Thermo-Calc software package. The AlN particles were observed by field-emission scanning electron microscopy (FESEM), and the amount of AlN precipitations was detected by electron probe microanalysis (EPMA). Based on the research results, it was found that the average grain size of austenite in the test steel increased continuously with the increase of temperature and holding time. Furthermore, the abnormal growth of austenite occurred in the test steel at 950°C, and the heating temperature affected the austenite grain size more significantly. In addition, the decline in the amount of AlN second-phase particle in the test steel, which weakened the "pinning" effect on austenite grain boundaries, resulted in abnormal growth and the development of mixed austenite grain structures. The prediction model for describing the austenite grain growth of medium-carbon alloy steel during heating was established by regression analysis of the experimental data, and the model was verified to be highly accurate.

Keywords: alloy steel; austenite grain; AlN; growth model

1. Introduction

Nowadays, higher standards of all kinds of steel properties are required. One method of improving the properties is to control the steel microstructure. The austenite grain size significantly influences the microstructure and properties of steel after cooling [1–3]. Generally, fine austenite grain size leads to higher strength, better ductility, and higher toughness [4–9]. To find out the appropriate methods to control the austenite grain size, several studies have been conducted on austenite grain growth [10–34]. Many researchers concentrate on the mechanism of austenite growth, and through the studies, the mechanism has been explained and understood from thermodynamics and kinetics factors, such as energy and diffusion. The driving force of the growth is the potential difference between these grains, which is dependent on the grain size. Because of the difference, the overall grain boundary area of the material tends to reduce, causing movements of grain boundaries. The grain boundary area is the main source of energy in the grain growth process [12–13,33–36]. Controlling the grain boundaries movements is the final way to obtain fine austenite grains.

Microalloyed additions, such as vanadium, niobium, titanium, and aluminum, are increasingly being employed to control austenite grain growth. These mircoalloyed elements become second-phase particles by combining with nitrogen or carbon. The second-phase particles which precipitate at the grain boundaries have a great "pinning" effect on grain boundaries, hindering the movements of boundaries [14–17,21–23]. The pinning mechanism between the grain boundary and the second-phase particle is largely due to the reduction of the grain boundary area, and hence reduction of energy, when the grain boundary intersects the second-phase particles. Any movement of the grain boundaries away from the particle can result in an increase of local energy and exert a drag effect on the migrating boundaries. The binding force between particles and boundaries is greater than that available by thermal activation [23]. Many studies have shown that the

Corresponding author: Yan-ping Bao E-mail: baoyp@ustb.edu.cn

pinning effect varies with size and number of second-phase particles [23–27]. The austenite grain size is better controlled using a large number of fine second-phase particles.

Many researchers have also established prediction models of austenite grain growth [31–32,35–45], the common models being Beck model [37], Hillert model [38], Arrhenius model [39], and Sellars model [40]. The Beck and Hillert models consider only one factor that influences the austenite average grain size, while Arrhenius and Sellars models contain more aspects.

In this study, the test material is medium-carbon alloy steel with aluminum additions, which is an alloy structural steel used for manufacturing various high-strength bolts [46]. The material is required to have superior properties such as yield strength, tensile strength, toughness. Accordingly, austenite grain size is one of the standards for the quality inspection of this steel [47]. By related experiments and analyses, the effects of heating temperature and holding time on the grain growth behavior of austenite in the test steel were investigated. In addition, the essential factors of abnormal growth and mixed second-phase particles (AlN) affecting the austenite growth were detected by combining electron probe microanalysis (EPMA) with wavelength dispersive spectrometry, and observed by combining field-emission scanning electron microscopy (FESEM) with energy dispersive spectrometry (EDS). Furthermore, the grain growth model of the test steel was established on the basis of the experimental results and Arrhenius model.

2. Experimental

The chemical composition of the test steel is given in Table 1. The dimension of the experimental specimens machined from as-received test steel is 15.0 mm × 15.0 mm × 15.0 mm. The experiment was conducted considering two perspectives: heating temperature and holding time, and thus was divided into two groups. The heat treatment was carried out in an SRJX-8-13 electric furnace, as shown in Fig. 1. In group one, the specimens were individually heated to 850, 900, 950, 1000, 1050, and 1100°C, and soaked for 30 min at corresponding temperatures. Then, the specimens were quenched in water to preserve the austenite microstructure grain boundaries. Subsequently, the specimens were heated to 230°C for 20 min [19] and cooled in air to room temperature. In group two, the specimens were heated to 950°C and separately held for 30, 60, 90, 120, and 150 min. Then, as in group one, they were heated to 230°C for 20 min and cooled in air to room temperature. After the heat treatment process, the specimens were polished and etched for 60 to 90 s in a 60°C aqueous solution of saturated picric acid and three drops of detergents. The austenite grains were observed on a TOUPCAM UCMOS03100KPA microscope. The average austenite grain sizes were measured using the standard test methods described in ASTM E 112 [34]. In addition, 95% confidence interval of austenite grain size was considered.

The concentration distribution of elements in the tested samples was analyzed by an electron probe microanalyzer equipped with wavelength dispersive spectrometers at an operating condition of 15.00 kV, 100 nA, and step size of 0.5 μm. To better characterize the AlN in the test steel, the samples were demagnetized before the morphologies of second-phase particles were directly observed in the steel samples by a field-emission scanning electron microscope equipped with an energy dispersive spectrometer. A voltage of 20.00 kV and current of 7.0 μA were used.

Table 1. Chemical composition of the test steel wt%

C	Si	Mn	P	S	Al	Cr	N
0.40	0.17	0.66	0.01	0.0044	0.041	0.97	0.0061

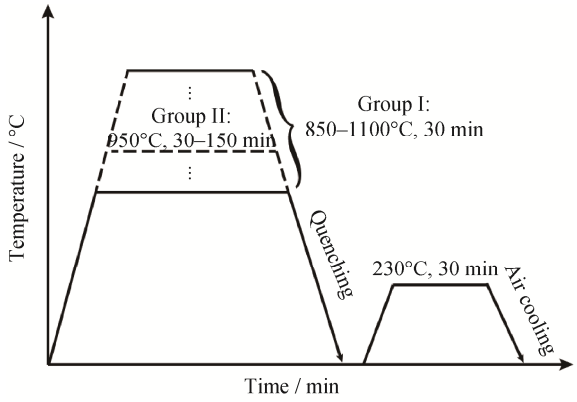

Fig. 1. Heat treatment processes of test steel.

3. Results and discussion

3.1. Effect of heating temperature on the average austenite grain size

Fig. 2 shows the morphologies of austenite grains in the test steel at different heating temperatures and a soaking time of 30 min. The austenite grain growth behavior of the test steel within the experimental temperature range can be divided into two stages: the first stage is from 850 to 950°C (Figs. 2(a)–2(c)). The austenite grains grew slowly at this stage, and the average size was 11 to 19 μm; thus, the first stage is defined as normal grain growth [11], and these grains can be categorized as ultrafine grains. In addition, the austenite grain size was relatively uniform. When the tem-

perature was above 950°C and up to 1000°C, the austenite growth developed into the second stage. At this stage, the austenite grain size increased rapidly (Fig. 2(d)). Consequently, abnormal grain growth occurred at 950°C, while mixed grain structures appeared at 1000°C in the test steel. At 1100°C, the average austenite grain size started to exceed 75 μm, but the size tended to be uniform when the temperature was above 1000°C. In order to show that the changes of proportion of different grain sizes in the heating process, statistical analyses of austenite grain size at typical temperatures (coarsening and two closest temperatures to it) are given in Fig. 3. From 850 to 1100°C, the average austenite grain size of the test steel grew from 11.52 ± 1.76 to 75.31 ± 2.71 μm. Fig. 4 shows more distinctly the effect of heating temperature on the average austenite grain size of the test steel. Meanwhile, for comparison, the results of other studies [10,48–51] which explored steels with similar or related composition as the test steel are shown in Fig. 4.

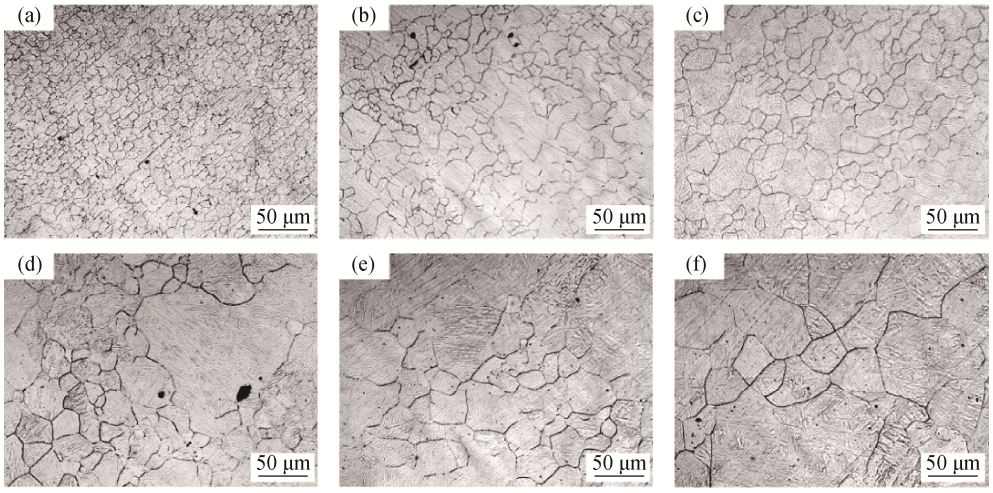

Fig. 2. Morphologies of austenite grains in test steel heated at different temperatures for 30 min: (a) 850°C; (b) 900°C; (c) 950°C; (d) 1000°C; (e) 1050°C; (f) 1100°C.

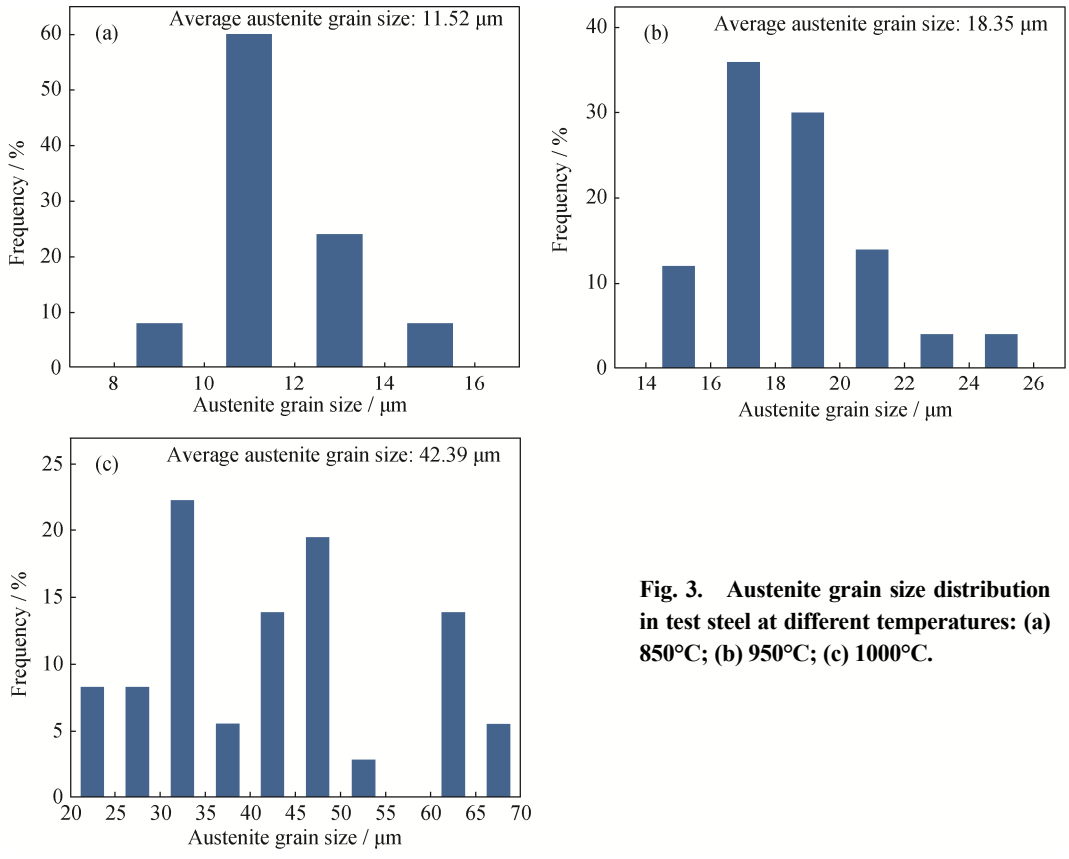

Fig. 3. Austenite grain size distribution in test steel at different temperatures: (a) 850°C; (b) 950°C; (c) 1000°C.

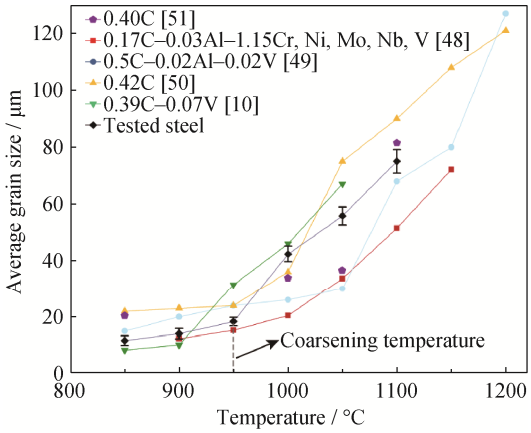

Fig. 4. Effect of heating temperature on the average austenite grain size of test steel and other previous studies [10,48–51].

3.2. Effect of holding time on average austenite grain size

Fig. 5 shows the morphologies of austenite grains in the test steel with different holding times at 950°C. Fig. 6(a) shows the effect of holding time on the average austenite grain size of the test steel. Compared with the heating temperature, the holding time had a lesser effect, and resulted in a smaller change of the average austenite grain size. Statistical analyses of austenite grain size at typical temperatures are given in Figs. 6(b) and 6(c). At the same heating temperature, the average austenite grain size of the test steel grew constantly with increase in holding time. The range of grain size was from 16.18 ± 0.46 to 31.70 ± 1.40 μm. Compared with the rapid growth at coarsening temperature, the changes of average austenite grain size were almost the same when holding time increases every 30 min. When the holding time reached 120 min, mixed grain structures appeared.

3.3. Effect of AlN on austenite grain size

According to the chemical composition of the test steel, Al is present in the steel. Aluminium combines with N to form second-phase particles AlN. These particles can hinder the movement of austenite grain boundaries [12–13]. To investigate the effect of second-phase particles on the austenite grain growth of the test steel, a phase diagram calculation was conducted using PLOY3 and POST module of Thermo-Calc. Fig. 7 shows the main precipitated phases of test steel at different experiment temperatures. The precipitated phases of the test steel changed with increase in temperature. When the temperature was 949°C, the AlN particles were almost completely dissolved, and Al atom was present in the form of a solid solution in the matrix. Tiny AlN particles in the steel precipitated at the austenite grain boundaries contributed to the pinning of adjacent austenite; thus, the movement of the austenite grain boundaries was hindered, and the austenite grain growth was effectively controlled. Fig. 8 is a schematic diagram illustrating the process of austenite coarsening and mixed grain structures development. From 850 to 950°C, the first dissolved AlN second-phase particles lost the original pinning effect, which means these particles no more hindered the movements of austenite boundaries at this area. Consequently, austenite grains grew by the influence of temperature. On the contrary, undissolved AlN second-phase particles exerted the pinning effect on austenite grains as before, leading to an inconspicuous change of austenite grain size within this area. The above descriptions explain why the coarsening temperature of the specimens was 950°C and mixed grains appeared at

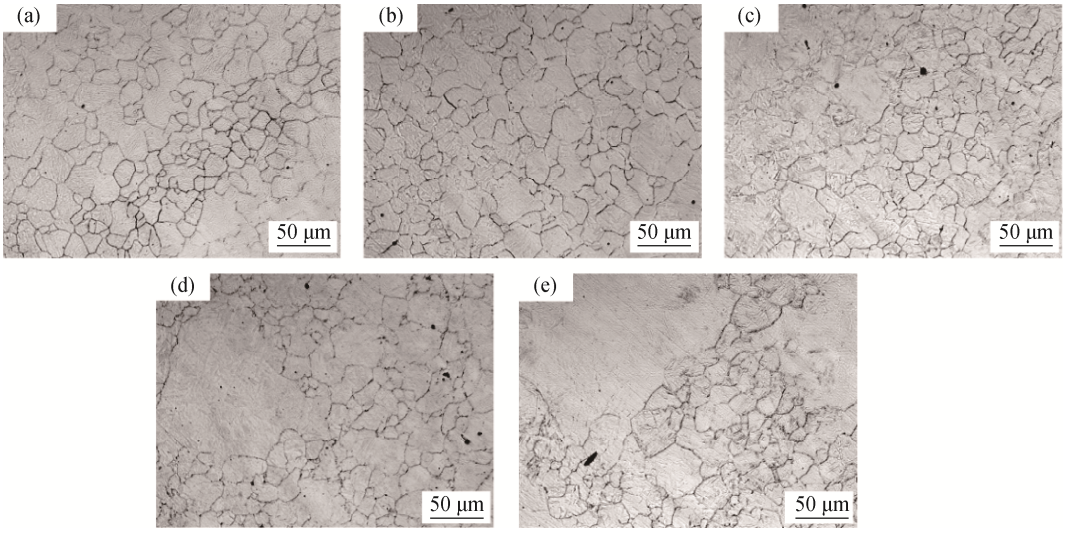

Fig. 5. Morphologies of test steel at heating temperature of 950°C with different holding times: (a) 30 min; (b) 60 min; (c) 90 min; (d) 120 min; (e) 150 min.

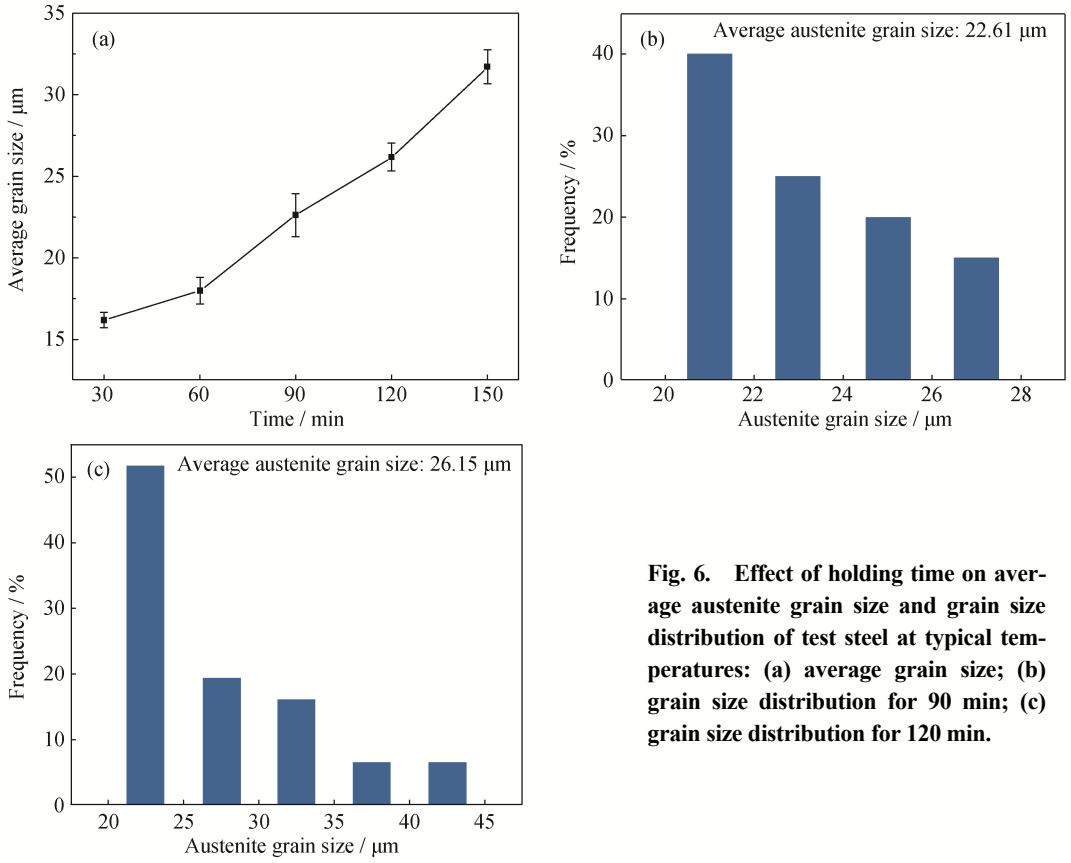

Fig. 6. Effect of holding time on average austenite grain size and grain size distribution of test steel at typical temperatures: (a) average grain size; (b) grain size distribution for 90 min; (c) grain size distribution for 120 min.

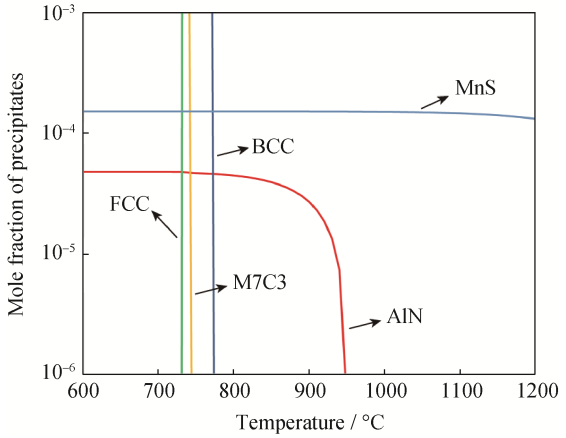

Fig. 7. Main precipitates in the range of the experiment temperature.

1000°C. As the temperature was continuously raised, austenite grain growth was no longer hindered because most AlN particles were dissolved in the steel; therefore, the austenite grains grew continuously by the influence of the heating temperature. The mixed grain structures disappeared as the grain size approached average.

Fig. 9 shows the mapping results of the precipitated phase in the test steel at 850 and 950°C using EPMA. As seen from Fig. 9, the locations of Al and N correspond well. When the heating temperature was 850°C, there was a higher mass fraction of Al and N at the austenite grain boundaries, especially at the cross boundaries of three austenite. At 950°C, the mass fraction of Al and N was much lower than that at 850°C. For further investigation, the volume fraction

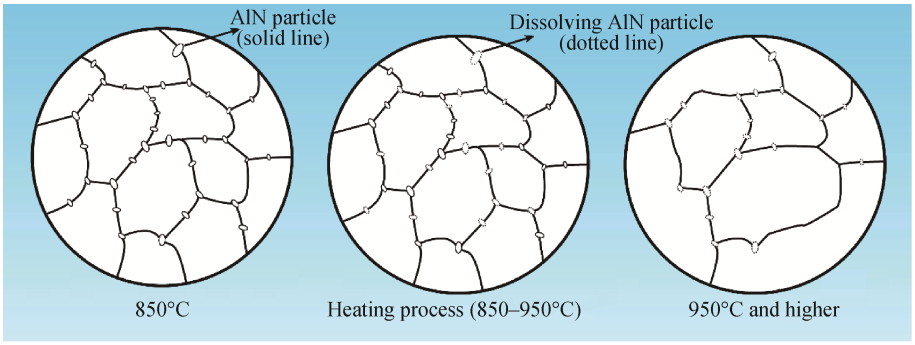

Fig. 8. Austenite coarsening and mixed grain structures development process.

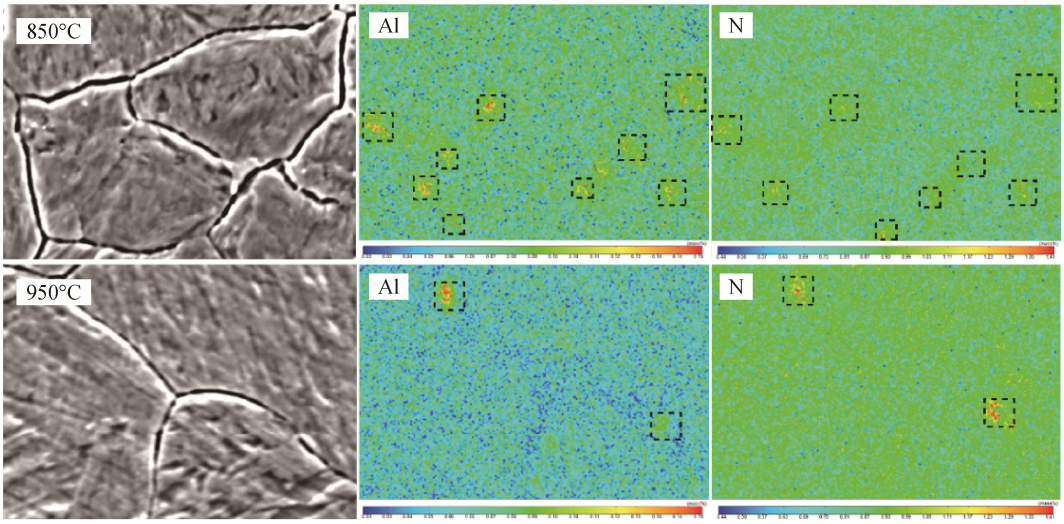

Fig. 9. EPMA mapping results of phases precipitating in test steel at 850 and 950°C.

of AlN in the test steel was calculated by Eq. (1) [9], and the calculation result is shown in Fig. 10.

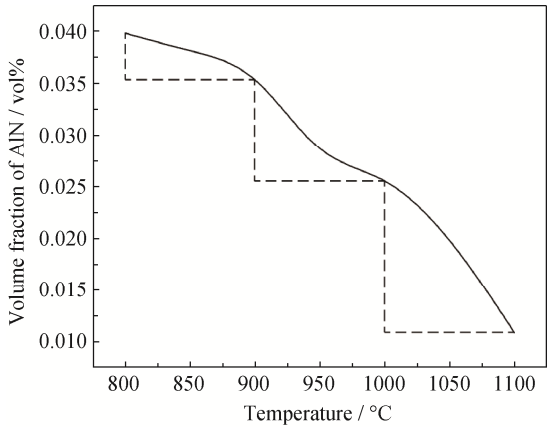

Fig. 10. Volume fraction of AlN at different temperatures.

$$f_{\mathrm{AlN}} = \frac{V_{\mathrm{AlN}}}{V_{\mathrm{AlN}} + V_{\mathrm{Fe}}} \tag{1}$$

$$V_{\mathrm{AlN}} = \frac{m_{\mathrm{AlN}}}{\rho_{\mathrm{AlN}}} \tag{2}$$

$$V_{\mathrm{Fe}} = \frac{m_{\mathrm{Fe}}}{\rho_{\mathrm{Fe}}} \tag{3}$$

$$m_{\mathrm{AlN}} = m_{\mathrm{Al}} + m_{\mathrm{N}} \tag{4}$$

$$m_{\mathrm{Fe}} = 1 - m_{\mathrm{AlN}} \tag{5}$$

$$m_{\mathrm{AlN}} = [\mathrm{Al}]_{\mathrm{p}} \tag{6}$$

where f_{AlN} is volume fraction of AlN precipitates, V_{AlN} and V_{Fe} are volumes of Al precipitates and Fe in steel. m_{AlN} is the mass of AlN precipitated in AlN-Fe matrix. ρ_{AlN} is the density of AlN. m_{Fe} is mass of Fe in AlN-Fe matrix and ρ_{Fe} is the density of Fe. m_{Al} is mass of Al atoms in AlN precipitations and m_{N} is mass of N atoms in AlN precipitations.

As shown in Fig. 10, the volume fraction of AlN in 850 and 950°C were 0.040vol% and 0.029vol% respectively. There was a sharp decline from 900 to 1000°C, which conforms to the experiment results. Furthermore, AlN precipitates were observed by FESEM as AlN can be characterized *in situ* at grain boundaries. Quantities of 100-nanoscale AlN particles were precipitated at the austenite grain boundaries. Fig. 11 shows FESEM images and the corresponding EDS spectra of AlN precipitates picked from random positions of the specimens. Both the distribution and fraction of AlN can further explain the grain coarsening and mixed grain structures. The quantity of AlN particles reduced greatly, which weakened the pinning effect of second-phase on austenite boundaries and led to the austenite grain coarsening.

3.4. Growth model of austenite grain growth

The heating temperature and holding time are the two external factors that have the greatest influence on the austenite growth behavior, and the two factors play a common role in the austenite grain growth. Regardless of the initial austenite grain size, Arrhenius model [39], shown as Eq. (7), was chosen to describe the austenite grain growth behavior of the test steel.

$$D = At^{n}\exp(-\frac{Q}{RT}) \tag{7}$$

where D is the average austenite grain size (μm), t is the holding time (s), Q is the activation energy for grain growth ($\mathrm{J\cdot mol^{-1}}$), R is the gas constant (8.314 $\mathrm{J\cdot mol^{-1}\cdot K^{-1}}$), T is the absolute heating temperature (K), n is grain growth index, A is the material constants.

To determine the value of constants A and Q, natural logarithm was taken on both sides of Eq. (7), and the result is expressed as Eq. (8). Fig. 12(a) shows the relationship between ln$D$ and ln$t$. The grain growth index n was obtained by linear regression. The greater n is, the faster the grains grow [10].

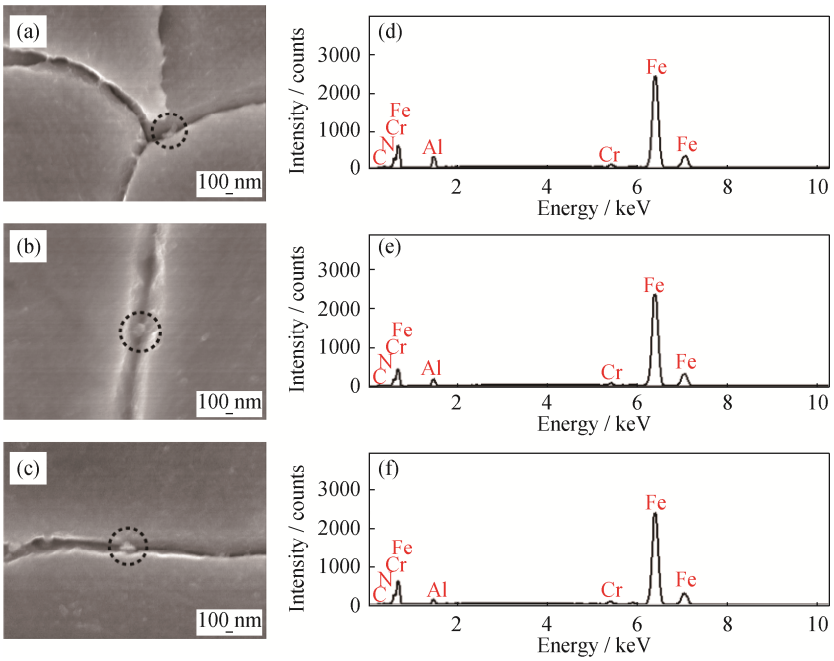

Fig. 11. FESEM images (a, b, and c) of AlN particles in different positions of austenite grain boundaries and EDS spectras (d, e, and f) for (a), (b), and (c), respectively.

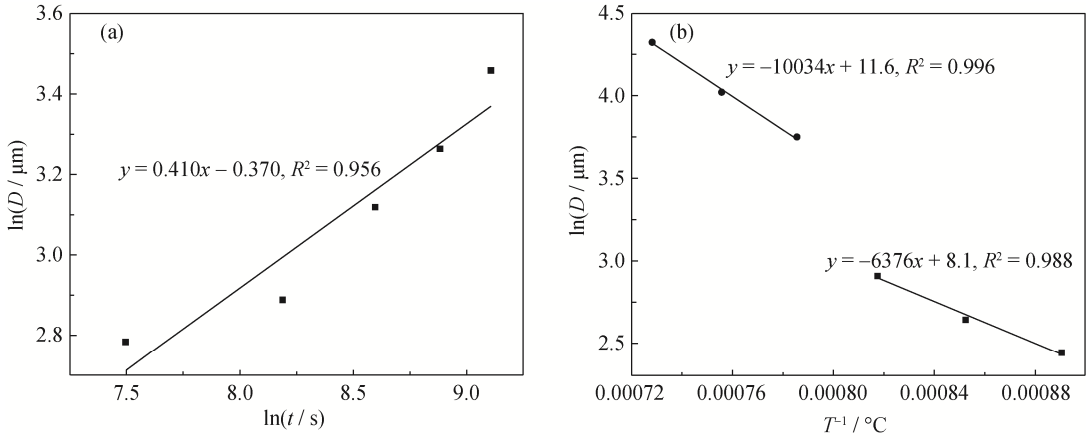

Fig. 12. Linear fitting curve of (a) ln$D$–ln$t$ and (b) ln$D$–T^{-1}.

$$\ln D = -\frac{Q}{RT} + \ln A + n\ln t \quad (8)$$

Fig. 12(b) shows the result of linear regression based on Eq. (8). There is an obvious difference between the austenite grain growth rates at temperatures higher and lower than the coarsening temperature. To obtain a more accurate model, the two stages of austenite grain growth which are distinguished by the coarsening temperature, were linearly fitted [19,48]. Consequently, the values of Q at the two stages were 53010 J·mol^{-1} and 83423 J·mol^{-1}. The corresponding values of A at the two stages were 154 and 5158, which were obtained by substituting the values of Q and n into Eq. (8). Finally, the models of the two stages of austenite grain growth, at temperatures higher and lower than the coarsening temperature, are described as follows:

$$D = 154t^{0.41}\exp(-\frac{53010}{RT}),\ (850\text{–}950°C) \quad (9)$$

$$D = 5158t^{0.41}\exp(-\frac{83423}{RT}),\ (1000\text{–}1100°C) \quad (10)$$

The austenite grain sizes predicted using the above growth models were compared with the measured sizes of test steel (Fig. 13). D_c and D_m are diameters obtained by growth models and experiment measure respectively. The red line of which slope is 0.97 in Fig. 13 is the result of linear fitting. The high degree of coincidence illustrates the high accuracy of the growth models.

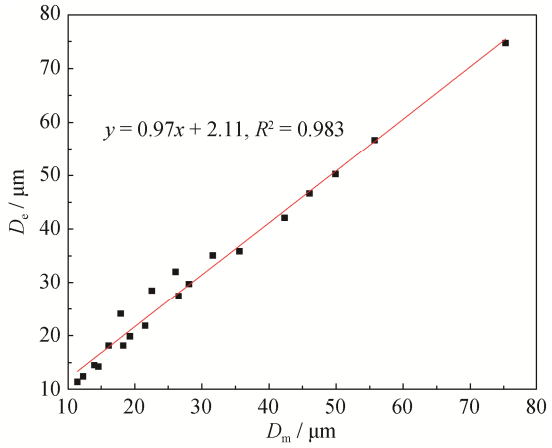

Fig. 13. Comparison of the calculated results D_c and experimental results D_m.

4. Conclusions

(1) In this study, the austenite grain size of medium-carbon alloy steel increased with the increase of heating temperature and holding time. The effect of heating temperature on austenite grain growth was greater than that of holding time. The coarsening temperature of the test steel was 950°C. The austenite grains grew slowly between 850°C–950°C, and grew rapidly at above 950°C. Mixed grain structures appeared at 1000°C.

(2) The amount of AlN second-phase particles greatly reduced when the temperature was raised to 950°C, which weakened or nearly eliminated the pinning effect of AlN particles on austenite grain boundaries. That explains why the austenite grain coarsening temperature of test steel was 950°C.

(3) The growth models of austenite grain in the test steel were established using the mathematical regression analysis, and are defined as follows:

$$D = 154t^{0.41}\exp(-\frac{53010}{RT}),\ (850\text{–}950°C);$$

$$D = 5158t^{0.41}\exp(-\frac{83423}{RT}),\ (1000\text{–}1100°C).$$

Acknowledgement

This work was financially supported by the National Natural Science Foundation of China (No. 51774037).

References

[1] M. Maalekian, R. Radis, M. Militzer, and A. Moreau, and W.J. Poole, *In situ* measurement and modelling of austenite grain growth in a Ti/Nb microalloyed steel, *Acta Mater.*, 60(2012), No. 3, p. 1015.

[2] J. Fernández, S. Illescas, and J.M. Guilemany, Effect of microalloying elements on the austenitic grain growth in a low carbon HSLA steel, *Mater. Lett.*, 61(2007), No. 11-12, p. 2389.

[3] J. Moon, J. Lee, and C. Lee, Prediction for the austenite grain size in the presence of growing particles in the weld HAZ of Ti-microalloyed steel, *Mater. Sci. Eng. A*, 459(2007), No. 1-2, p. 40.

[4] R. Dippenaar, C. Bernhard, S. Schider, and G. Wieser, Austenite grain growth and the surface quality of continuously cast steel, *Metall. Mater. Trans. B*, 45(2014), No. 2, p. 409.

[5] J.J. Lewandowski and A.W. Thompson, Effects of the prior austenite grain size on the ductility of fully pearlitic eutectoid steel, *Metall. Trans. A*, 17(1986), No. 3, p. 461.

[6] Y. Prawoto, N. Jasmawati, and K. Sumeru, Effect of prior austenite grain size on the morphology and mechanical properties of martensite in medium carbon steel, *J. Mater. Sci. Technol.*, 28(2012), No. 5, p. 461.

[7] H. Zhao and E.J. Palmiere, Erratum to: Effect of austenite deformation on the microstructure evolution and grain refinement under accelerated cooling conditions, *Metall. Mater. Trans. A*, 48(2017), No. 10, p. 5164.

[8] J. Han, A.K. da Silva, D. Ponge, D. Raabe, S.M. Lee, Y.K. Lee, S.I. Lee, and B. Hwang, The effects of prior austenite grain boundaries and microstructural morphology on the impact toughness of intercritically annealed medium Mn steel, *Acta Mater.*, 122(2017), p. 199.

[9] X.P. Ma, B. Langelier, B. Gault, and S. Subramanian, Effect of Nb addition to Ti-bearing super martensitic stainless steel on control of austenite grain size and strengthening, *Metall. Mater. Trans. A*, 48(2017), No. 5, p. 2460.

[10] S.S. Zhang, M.Q. Li, Y.G. Liu, J. Luo, and T.Q. Liu, The growth behavior of austenite grain in the heating process of 300M steel, *Mater. Sci. Eng., A*, 528(2011), No. 15, p. 4967.

[11] X.G. Zhang, K. Matsuura, and M. Ohno, Abnormal grain growth in austenite structure reversely transformed from ferrite/pearlite-banded structure, *Metall. Mater. Trans. A*, 45(2014), No. 10, p. 4623.

[12] O. Flores and L. Martinez, Abnormal grain growth of austenite in a V–Nb microalloyed steel, *J. Mater. Sci.*, 32(1997), No. 22, p. 5985.

[13] L.J. Cuddy and J.C. Raley, Austenite grain coarsening in microalloyed steels, *Metall. Trans. A*, 14(1983), No. 10, p. 1989.

[14] C.M. Enloe, K.O. Findley, and J.G. Speer, Austenite grain growth and precipitate evolution in a carburizing steel with combined niobium and molybdenum additions, *Metall. Mater. Trans. A*, 46(2015), No. 11, p. 5308.

[15] M. Militzer, E.B. Hawbolt, T.R. Meadowcroft, and A. Giumelli, Austenite grain growth kinetics in Al-killed plain carbon steels, *Metall. Mater. Trans. A*, 27(1996), No. 11, p. 3399.

[16] H. Pous-Romero, I. Lonardelli, D. Cogswell, and H.K.D.H. Bhadeshia, Austenite grain growth in a nuclear pressure vessel steel, *Mater. Sci. Eng. A*, 567(2013), p. 72.

[17] L. Zhang and T. Kannengiesser, Austenite grain growth and microstructure control in simulated heat affected zones of microalloyed HSLA steel, *Mater. Sci. Eng. A*, 613(2014), p. 326.

[18] V.I. Savran, S.E. Offerman, and J. Sietsma, Austenite nucleation and growth observed on the level of individual grains by three-dimensional X-Ray diffraction microscopy, *Metall. Mater. Trans. A*, 41(2010), No. 3, p. 583.
[19] S.F. Tao, F.M. Wang, G.L. Sun, Z.B. Yang, and C.R. Li, DICTRA simulation of holding time dependence of NbC size and experimental study of effect of NbC on austenite grain growth, *Metall. Mater. Trans. A*, 46(2015), No. 8, p. 3670.
[20] A. Ray, S.K. Ray, and S.R. Mediratta, Effect of carbides on the austenite grain growth characteristics in 1Cr–1C and 6Cr–1Mo–1C steels, *J. Mater. Sci.*, 25(1990), No. 12, p. 5070.
[21] K. Zhu and Z.G. Yang, Effect of magnesium on the austenite grain growth of the heat-affected zone in low-carbon high-strength steels, *Metall. Mater. Trans. A*, 42(2011), No. 8, p. 2207.
[22] A.M. Elwazri, S. Yue, and P. Wanjara, Effect of prior-austenite grain size and transformation temperature on nodule size of microalloyed hypereutectoid steels, *Metall. Mater. Trans. A*, 36(2005), No. 9, p. 2297.
[23] M.A. Bepari, Effects of second-phase particles on coarsening of austenite in 0.15 Pct carbon steels, *Metall. Trans. A*, 20(1989), No. 1, p. 13.
[24] S. Sarkar, A. Moreau, M. Militzer, and W.J. Poole, Evolution of austenite recrystallization and grain growth using laser ultrasonics, *Metall. Mater. Trans. A*, 39(2008), No. 4, p. 897.
[25] S. Maropoulos, S. Karagiannis, and N Ridley, Factors affecting prior austenite grain size in low alloy steel, *J. Mater. Sci.*, 42(2007), No. 4, p. 1309.
[26] P.A. Manohar, D.P. Dunne, T. Chandra, and C.R. Killmore, Grain growth predictions in microalloyed steels, *ISIJ Int.*, 36(1996), No. 2, p. 194.
[27] Q.Y. Sha and Z.Q. Sun, Grain growth behavior of coarse-grained austenite in a Nb–V–Ti microalloyed steel, *Mater. Sci. Eng. A*, 523(2009), No. 1-2, p. 77.
[28] X.L. Wan, K.M. Wu, G. Huang, R. Wei, and L. Cheng, *In situ* observation of austenite grain growth behavior in the simulated coarse-grained heat-affected zone of Ti-microalloyed steels, *Int. J. Miner. Metall. Mater.*, 21(2014), No. 9, p. 878.
[29] Y. Gu, P. Tian, X. Wang, X.L. Han, B. Liao, and F.R. Xiao, Non-isothermal prior austenite grain growth of a high-Nb X100 pipeline steel during a simulated welding heat cycle process, *Mater. Des.*, 89(2016), p. 589.
[30] Ö.N. Doğan, G.M. Michal, and H.W. Kwon, Pinning of austenite grain boundaries by AIN precipitates and abnormal grain growth, *Metall. Trans. A*, 23(1992), No. 8, p. 2121.
[31] S.J. Lee and Y.K. Lee, Prediction of austenite grain growth during austenitization of low alloy steels, *Mater. Des.*, 29(2008), No. 9, p. 1840.
[32] Y.W. Xu, D. Tang, Y. Song, and X.G. Pan, Prediction model for the austenite grain growth in a hot rolled dual phase steel, *Mater. Des.*, 36(2012), p. 275.
[33] K. Matsuura and Y. Itoh, Analysis of the effect of grain size distribution on grain growth by computer simulation, *ISIJ Int.*, 31(1991), No. 4, p. 366.
[34] K. Pawlak, B. Białobrzeska, and Ł. Konat, The influence of austenitizing temperature on prior austenite grain size and resistance to abrasion wear of selected low-alloy boron steel, *Arch. Civ. Mech. Eng.*, 16(2016), No. 4, p. 913.
[35] Y. Vertyagina, M. Mahfouf, and X. Xu, 3D modelling of ferrite and austenite grain coarsening using real-valued cellular automata based on transition function, *J. Mater. Sci.*, 48(2013), No. 16, p. 5517.
[36] Y. Vertyagina and M. Mahfouf, A 3D cellular automata model of the abnormal grain growth in austenite, *J. Mater. Sci.*, 50(2015), No. 2, p. 745.
[37] P.A. Beck, J.C. Kremer, and L.J. Demer, Grain growth in high purity aluminum, *Phys. Rev.*, 71(1947), No. 8, p. 555.
[38] M. Hillert, On the theory of normal and abnormal grain growth, *Acta Metall.*, 13(1965), No. 3, p. 227.
[39] E. Anelli, Application of mathematical modelling to hot rolling and controlled cooling of wire rods and bars, *ISIJ Int.*, 32(1992), No. 3, p. 440.
[40] C.M. Sellars and J.A. Whiteman, Recrystallization and grain growth in hot rolling, *Met. Sci.*, 13(1979), No. 3-4, p. 187.
[41] Y.X. Zhang, H.O. Zhang, G.L. Wang, and S.D. Hu, Application of mathematical model for microstructure and mechanical property of hot rolled wire rods, *Appl. Math. Modell.*, 33(2009), No. 3, p. 1259.
[42] Y. Fu and H. Yu, Application of mathematical modeling in two-stage rolling of hot rolled wire rods, *J. Mater. Process. Technol.*, 214(2014), No. 9, p. 1962.
[43] S. Uhm, J. Moon, C. Lee, J. Yoon, and B. Lee, Prediction model for the austenite grain size in the coarse grained heat affected zone of Fe–C–Mn steels: considering the effect of initial grain size on isothermal growth behavior, *ISIJ Int.*, 44(2004), No. 7, p. 1230.
[44] G.X. Jin, F.M. Wang, J. Fu, K.F. Li, and C.R. Li, Formation of martensite in 82B high carbon steel wire rod, *Trans. Mater. Heat Treat.*, 34(2013), No. 6, p. 62.
[45] S.F. Tao, F.M. Wang, Q.M. Yu, L.F. Sun, and G.Q. Chai, Effect of austenitizing temperature and holding time on austenite grain size of EQ70 steel, *Trans. Mater. Heat Treat.*, 34(2013), No. 11, p. 42.
[46] D.F. Hu and M. Chen, Practice of producing ML40Cr cold heading wire rod by process of 30 t BOF-billet continuous casting, *J. Mater. Metall.*, 10(2011), No. 3, p. 164.
[47] L.Z. Wu, J. Chen, and H.B. Zhang, Dynamic recrystallization of austenite and grain refinement in 40Cr Steel, *J. Shanghai Jiaotong Univ.*, 42(2008), No. 5, p. 786.
[48] R.T. Xiao, H. Yu, and P. Zhou, Austenite grain growth behavior of Q1030 high strength welded steel, *Int. J. Miner. Metall. Mater.*, 19(2012), No. 8, p. 711.
[49] S.W. Du, Y.T. Li, and Y. Zheng, Kinetics of austenite grain growth during heating and its influence on hot deformation of LZ50 steel, *J. Mater. Eng. Perform.*, 25(2016), No. 7, p. 2661.
[50] B. Jiang, M. Wu, H. Sun, Z.L. Wang, Z.G. Zhao, and Y.Z. Liu, Prediction model of austenite growth and the role of MnS inclusions in non-quenched and tempered steel, *Met. Mater. Int.*, 24(2018), No. 1, p. 15.
[51] F. Liu, G. Xu, Y.L. Zhang, H.J. Hu, L.X. Zhou, and Z.L. Xue, *In situ* observations of austenite grain growth in Fe–C–Mn–Si super bainitic steel, *Int. J. Miner. Metall. Mater.*, 20(2013), No. 11, p. 1060.